Experimental Cell Research **258,** 33–41 (2000)
doi:10.1006/excr.2000.4909, available online at http://www.idealibrary.com on IDEAL®

Human Dentin Production *in Vitro*

Imad About,*[,1] Marie-José Bottero,* Philippe de Denato,† Jean Camps,*
Jean-Claude Franquin,* and Thimios A. Mitsiadis*

**Laboratoire IMEB, Faculté d'Odontologie, Université de la Méditerranée, 13385 Marseille Cedex 5, France; and †LEM, CNRS, URA 235, Vandoeuvre les-Nancy, France*

The main hard tissues of teeth are composed of dentin and enamel, synthesized by the mesenchyme-derived odontoblasts and the epithelial-derived ameloblasts, respectively. Odontoblasts are highly differentiated post-mitotic cells secreting the organic matrix of dentin throughout the life of the animal. Pathological conditions such as carious lesions and dental injuries are often lethal to the odontoblasts, which are then replaced by other pulp cells. These cells are able to differentiate into odontoblast-like cells and produce a reparative dentin. In this study we reproduced this physiological event in an *in vitro* culture system using pulps of human third molars. Pulp cells cultured in presence of β-glycerophosphate formed mineralization nodules, which grew all over the culture period. The immunohistochemical study revealed that, as odontoblasts, pulp cells contributing to the nodule formation express type I collagen, osteonectin, and nestin. By the exception of nestin, these proteins are also detected in the nodules. The composition of the nodules was also analyzed by Fourier transform infrared microspectroscopy. The spectra obtained showed that both the organic and the mineral composition of the nodules have the characteristics of the human dentin and differ from those of enamel and bone. Taken together, these results show that both the molecular and the mineral characteristics of the human dentin matrix are respected in the *in vitro* culture conditions.

Key Words: **tooth; dentin; odontoblast; human; differentiation; culture.**

INTRODUCTION

During tooth development, inductive epithelial–mesenchymal interactions lead to the differentiation of ectomesenchymal pulp cells into odontoblasts. These cells express specific gene products that will form the highly mineralized extracellular matrix of dentin. Hydroxyapatite forms the main inorganic part of dentin while the organic components consist mostly of type I collagen [1]. Fewer amounts of noncollagenous proteins detected in the extracellular matrix of the bone such as decorin [2], biglycan [2], osteonectin [3], osteocalcin [4], osteopontin [5], bone sialoprotein [6], and dentin matrix protein-1 [7, 8] are also found in the dentin. However, two extracellular matrix proteins have been shown to be specific for the dentin matrix, the dentin sialoprotein (DSP) [9, 10] and the dentin phosphoprotein (DPP) [11, 12]. These two proteins are the result of a common transcript designated DSPP for the dentin sialophosphoprotein [13, 14]. In addition to these extracellular matrix proteins, several signaling molecules such as transforming growth factor beta (TGFβ), bone morphogenic proteins (BMPs), and fibroblast growth factors (FGFs) are captured in the dentin [15, 16].

In pathological conditions such as carious lesions, the secretory activity of the odontoblasts is stimulated to elaborate reactionary dentin. It has been suggested that this stimulation may be due to signaling molecules (i.e., TGFβ1, BMP-2) liberated from the dentin during demineralization [17, 18]. In contrast, deep cavity preparation leads to odontoblast disintegration. In this case, newly formed odontoblast-like cells, possibly originated from dental pulp fibroblasts [19, 20], that elaborate the reparative dentin [21–23] replace odontoblasts. The deposition of reparative dentin may increase *in vivo* by the application of signaling molecules as a pulp capping medication, particularly with TGFβ1 [24] and BMP-7 [25]. Thus, these molecules seem to be necessary to stimulate proliferation and differentiation of pulp cells [26, 27].

To better understand the mechanisms underlying the reparative dentin production *in vivo,* many attempts were carried out to reproduce the differentiation of pulp cells into odontoblast-like cells *in vitro.* Successful cultures of dental pulp cells have been reported earlier in rodents and bovines [28, 29]. More recently, it has been shown that cultured pulp cells of human deciduous tooth germs are also able to form mineralization nodules [30]. Although the mineraliza-

[1] To whom reprint requests should be addressed. Fax: (33) 4 91 80 43 43. E-mail: imad.about@odontologie.univ-mrs.fr.

0014-4827/00 $35.00

tion nodules seem to be composed of hydroxyapatites when examined by X-ray diffractometry, the characteristics and the exact nature of both the cells and the nodules were not determined.

This work was designed to establish a reproducible and simple method for the differentiation of human dental pulp cells into odontoblastes *in vitro* and determine the nature of the mineralization nodules both at the molecular and Fourier transform infrared spectral (FTIR) levels.

MATERIALS AND METHODS

For the preparation of the culture media, all materials were purchased from GIBCO BRL (Life Technologies, Inc., Grand Island, NY) unless otherwise precised. Minimum essential medium (MEM) was supplemented with 10% fetal bovine serum, 2 mM glutamine, 100 UI/ml penicillin, 100 μg/ml streptomycin (Biowhittaker, Gagny, France), and 0.25 μg/ml amphotericin B (Fungizone).

Teeth. All teeth used in this study were immature third molars extracted during normal treatment of 16-year-old patients. The teeth were all normal, freshly extracted, and used with the patients' informed consent.

Antibodies. Polyclonal antibodies against the type I collagen were purchased from Southern Biotechnology Associates, Inc. (Birmingham, AL). Monoclonal antibody to osteonectin was obtained from Takara Biochemicals (Takara Shuzo Co. Ltd, Shiga, Japan). Preparation and characterization of the polyclonal antibodies against nestin have been already described [31, 32].

Culture of dental pulp cells. Immediately after the extraction, the teeth were swabbed with 70% (v/v) alcohol and then washed with sterile phosphate-buffered saline (PBS, 0.01 M, pH 7.4). The teeth were then transferred into a laminar flow tissue culture hood in order to perform the rest of the procedures under sterile conditions. The apical part of the teeth was removed with sterile scalpels and the dental pulps were gently removed with forceps. Dental pulps were minced with scalpels and rinsed with PBS. Each dental pulp was divided into two groups: cultured without (control) or with β-glycerophosphate (βGP). In the control group, the explants were cultured in 100-mm-diameter culture dishes (Becton Dickinson Labware, Lincoln Park, NJ) in MEM. In the second group, the explants were cultured under the same conditions in the same medium supplemented with 2 mM β-glycerophosphate (Sigma). The cultures were maintained at 37°C in a humidified atmosphere of 5% CO_2, 95% air. The culture medium was changed every other day. Confluent cultures were collected by trypsinization (0.2% trypsin and 0.02% EDTA) and subcultured.

Culture of osteoblasts. Osteoblasts served as a control in this study. After stimulation [33], these cells were cultured in the same medium and conditions as dental pulp cells.

Histology. Cultures of cells which formed the mineralization nodules were fixed with 4% paraformaldahyde for 24 h and demineralized in 14% EDTA, pH 4.7, for 8 weeks. After demineralization, the cells were fixed again with 2.5% glutaraldehyde in sodium cacodylate buffer, 0.1 mol/L, pH 7.2, for 1 h at 4°C. After washes, the cells were dehydrated in graded series of ethanol and embedded in Epon 812. One-micrometer-thick sections were performed and stained with toluidin blue.

Von Kossa staining. After dental pulp cells were fixed with 70% ethanol for 1 h, the culture dishes were washed with distilled water and then they were treated with 1% $AgNO_3$ for 20 min. After they were washed with distilled water they were treated with 2.5% sodium thiosulfate for 5 min. The samples were then examined without counterstaining or after Mayer's hematoxylin counterstaining.

Immunohistochemistry. After 3 weeks of culture, the cells were fixed with 70% ethanol for 1 h at 4°C. The cells were permeabilized for 15 min with 0.5% Triton X-100 in PBS. Primary antibodies were diluted in PBS containing 0.1% bovine serum albumin (BSA). The incubation with primary antibodies was performed overnight at 4°C at the following concentrations: anti-collagen I antibodies were used at 40 μg/ml, and anti-osteonectin at 50 μg/ml. Anti-nestin antibody was diluted 1:1500 in PBS. The staining was revealed using the labeled streptavidin–biotin kit (LSAB; Dako Corp., Carpinteria, CA) according to the manufacturer's instructions. Glycergel was used as a mounting medium (Dako). Controls were performed by incubations with unrelated primary antibodies.

Mineralization study on cultured cells. The cells were plated at $3 \times 10^3/cm^2$ on sterile 10-mm-diameter calcium fluoride (CaF_2) coverslips (Sorem, Pau, France) placed in four-well tissue-culture plates (Nunclon, Nunc, Roskilde, Denmark). The coverslips were cultured in MEM (control) or in MEM supplemented with 2 mM β-glycerophosphate for 4 weeks. FTIR microspectroscopy examinations were carried out on CaF_2 coverslips fixed with absolute ethanol at 4°C for 1 h.

Mineralization study on tooth sections. The teeth were fixed in absolute ethanol for 1 week and then the enamel was eliminated with a bur. Unembedded dentin was serially sliced in the pulp–coronal axis into 4-μm-thick sections using a Jung Polycut E (Leica, Heidelberg, Germany). Each section was mounted on a CaF_2 coverslip for FTIR MS analysis. The sections from pre-dentin to dentin were examined with respect to their special feature, where nonmineralized matrix ends and mineralized matrix begins. A 20-μm^2 area was mapped at 50-μm increments proceeding distally along a 1000-μm line perpendicular to the mineralization front so that 20 spectra were obtained for each tooth. Among the 20 spectra analyzed, 3 were chosen for the comparative study with the mineralization obtained *in vitro*. The first spectrum corresponds to the nonmineralized matrix. The second correlates to the mineralization front, and the third to dentin. Similarly, enamel and bone sections were prepared for a comparative purpose.

Fourier transform infrared microspectroscopy. FTIR MS examinations were recorded in the transmission mode on a FTIR (Bruker IFS55) spectrometer (Bruker, Karlsrhue, Germany) equipped with narrow-band mercury cadmium telluride detector responsive from 600 to 4000 cm^{-1} coupled with an infrared microscope (A590, Bruker, Karlsrhue, Germany). FTIR MS analysis was performed at a spatial resolution of approximately 20 μm, with a spectral resolution of ± 2 cm^{-1}. The signal-to-noise ratios were greater than 1200. Interferences from atmospheric water and CO_2 were removed by appropriate spectral substraction techniques. Each spectrum was obtained under nitrogen purge by the coaddition of 200 interferograms. The resulting mean interferogram was treated by the Fourier mathematical algorithm in order to obtain the corresponding absorbency spectrum. Following a baseline definition, the relative mineral-to-matrix ratios were calculated as the ratio of the integrated area of the phosphate band (900–1200 cm^{-1}) to that of amide I band (1580–1705 cm^{-1}).

The decomposition of the bands in the 860–880 cm^{-1} region was made using the algorithm of Levenberg–Marquardt and the bands were essentially obtained using gaussian functions.

RESULTS

Dental Papilla Explants in Culture Dishes

Cell proliferation and adhesion of dental pulp cells were observed after 3 days of the explant culture. After a 3-week culture in the presence of β-glycerophosphate, regular and fiber-like structures started to ap-

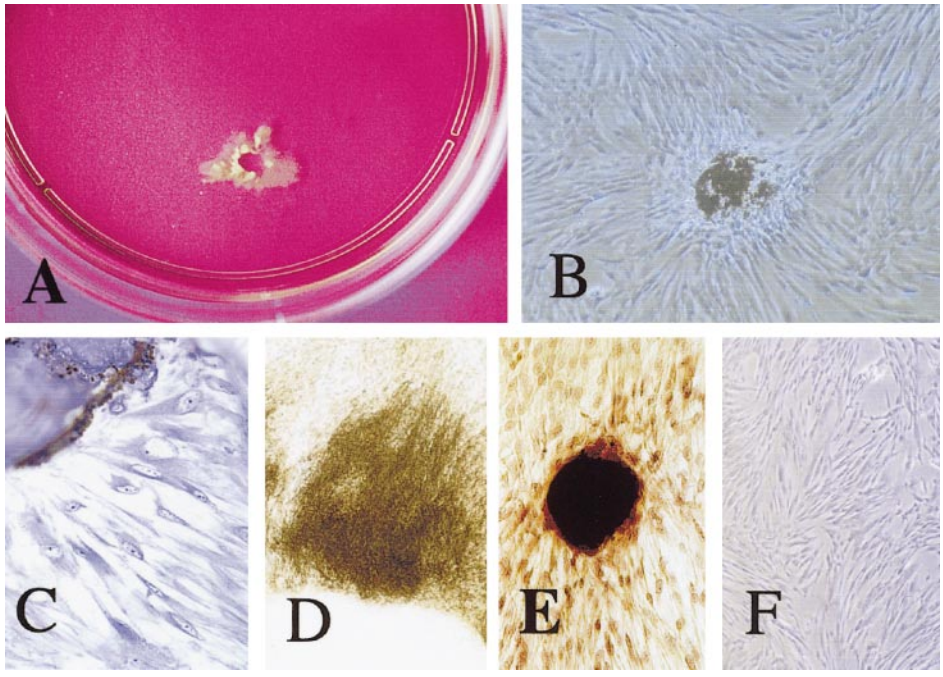

FIG. 1. Formation of mineralization nodules in human dental pulp explants *in vitro* after β-glycerophosphate treatment. (A) Formation of a mineralization nodule after 8 weeks of culture. (B) Phase contrast microscopy showing the formation of nodules after 3 weeks of treatment. (C) Histological section showing newly polarized cells in contact with the nodule and the absence of tubuli in the mineralized matrix (toluidine blue stain). (D) Mineralization organized in fiber-like structures. The secreted fibrillar matrix are oriented perpendicularly to the mineralization front. (E) Visualization of nodules after Von Kossa stain. (F) Control: human dental pulp explants cultured without β-glycerophosphate. Original magnifications: A, ×1; B, ×10; C, ×40; D, ×20; E, ×10; F, ×4.

pear from the explant border and extended toward the peripheral parts (Fig. 1). This was followed by the deposition of mineral crystals along and within the fibrous structures and this mineralization front continued to expand during the 8-week culture procedure (Figs. 1A and 1D). Furthermore, newly formed nodules were observed during this culture period (Fig. 1B). The cells in direct contact with the nodules exhibited a polarized morphology similar to that observed *in vivo.* Dentinal tubuli formation was not observed (Fig. 1C). Von Kossa staining showed that these nodules were calcium-positive (Fig. 1E). Cultures treated without β-glycerophosphate were used as a control; no mineralization was observed and the morphology of the cells was fibroblastic (Fig. 1F).

When the cells were subcultured, they quickly adhered to the culture surface and acquired a spindle-shape to polygonal morphology. After 2 weeks, the cells acquired a multilayered appearance at some areas that were the sites of the appearance of nodules. These mineralization nodules were visible after β-glycerophosphate treatment for 2 weeks and continued to grow and increase in size as long as the culture process was continued. Numerous nodules were observed on β-glycerophosphate-treated dishes, while no mineralization was observed in the control cultures.

Characterization of Dental Papilla Cells

Type I collagen immunoreactivity was strong and uniform in all β-glycerophosphate-treated cells. The expression of collagen I was also evident in the mineralization nodules (Figs. 2A–2C). Osteonectin (Figs. 2D and 2E) was expressed in these cells as well as in the nodules. However, the staining intensity was higher in cells contacting the mineralization nodules than the cells away from the nodules (Fig. 2D). Nestin was expressed in the dental pulp cells (Fig. 2F) but not in the osteoblasts (Fig. 2G). Immunostaining for nestin was more intense in the cells contacting the nodules (Fig. 2F). All controls where the cells were incubated with unrelated antibodies gave negative results (Fig. 2H).

FTIR-MS Examinations of the Mineralization in Vitro

The lower spectrum corresponds to control cultures where no mineralization is observed (Fig. 3A). The peaks correlating to the phosphate ions are completely absent. After the addition of βGP, the bands and peaks correlating to phosphate ions are observed (upper spectrum) at 872, 960, 1024, and 1095 cm^{-1}, and for the amides at 1550 and 1640–1650 cm^{-1}. The comparison of the spectra obtained *in vitro* to those obtained from

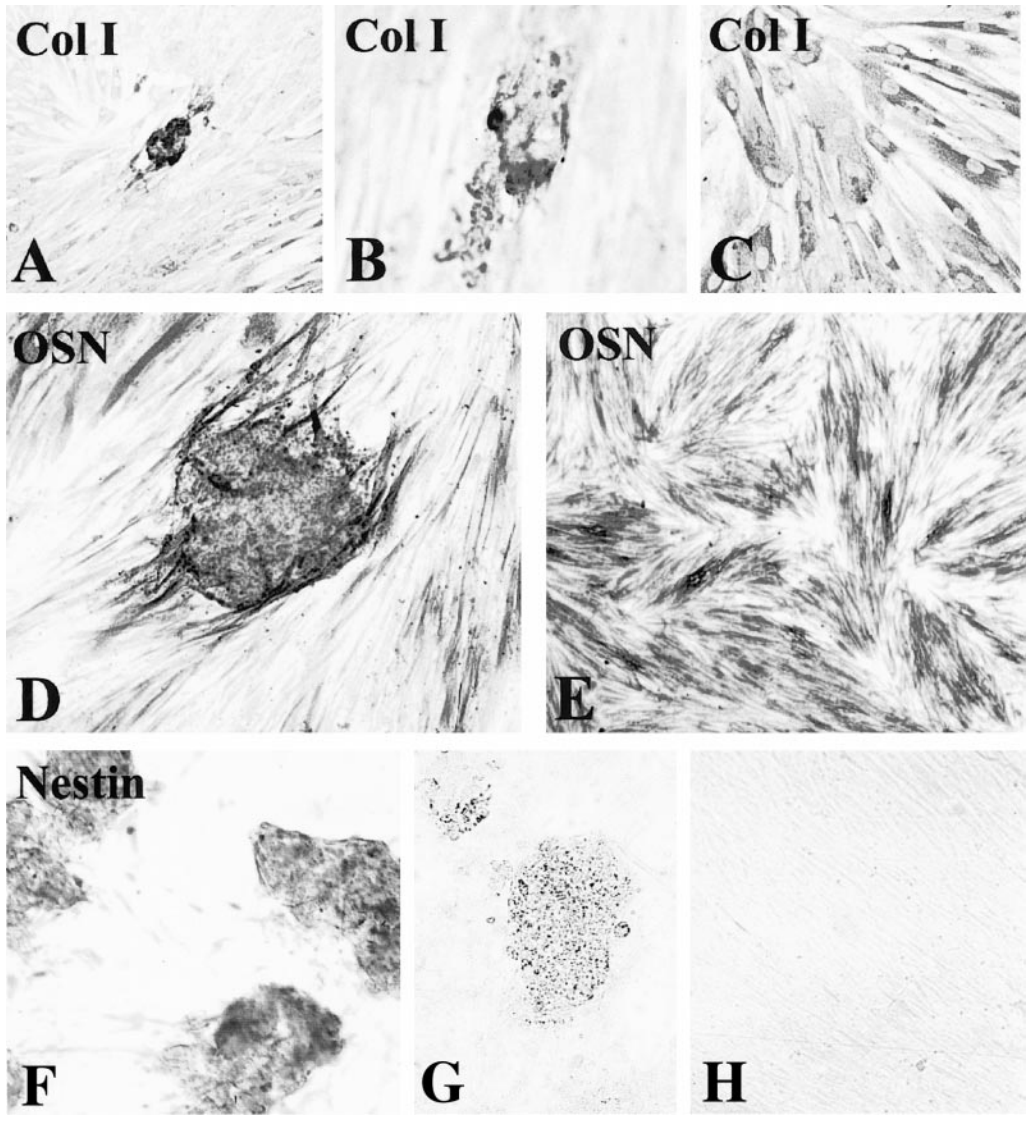

FIG. 2. Protein expression in human dental pulp explants after 3 weeks of culture with β-glycerophosphate. (A–C) Collagen I expression in dental papilla cells and in the mineralization nodules. (D, E) Osteonectin expression in the nodules (D) and in dental pulp cells (E). Note that osteonectin expression in cells contacting the nodules is stronger than in cells at a distance from the nodules (D). (F) Nestin expression in the dental papilla cells. The staining is absent from the mineralization nodules. (G) Control: the nestin staining is absent in human osteoblastic cells. (H) Control: the immunostaining is absent when the dental papilla cells were incubated with unrelated primary antibodies. Original magnifications: A, ×4; B, ×10; C, ×20; D, ×10; E, ×4; F, ×10; G, ×10; H, ×10.

the dentin *in vivo* shows a great analogy and the components are of the same types and located at the same positions (Table 1). The spectra show that the mineral-to-matrix ratio (Table 2) in βGP-treated cultures is higher than that obtained with bone and dentin.

The deconvolution of v_2 CO_3 band of the *in vitro* mineralization (Fig. 3B) is resolved in three major components at 864 cm^{-1} (shoulder), 872 cm^{-1}, and 880 cm^{-1} (shoulder).

FTIR MS Examinations of the Mineralization in Vivo

Dentin. The spectra of mineralization obtained *in vivo* show major differences. The lower spectrum corresponds to the organic matrix, where no mineralization is observed. In the middle spectrum, which corresponds to the mineralization front, the peaks of phosphate ions are observed at 872, 960, 1024, and 1095 cm^{-1}, and amides at 1550 and 1640–1650 cm^{-1}. In the upper spectrum, which corresponds to the dentin, an increase in the peaks and bands representing phosphate ions and amides at the same wave numbers is observed (Fig. 3C).

Hard tissues. The mineralization of dentin (upper spectrum) differs from those of the other tooth hard tissues (Fig. 3D). Enamel (intermediate spectrum) ex-

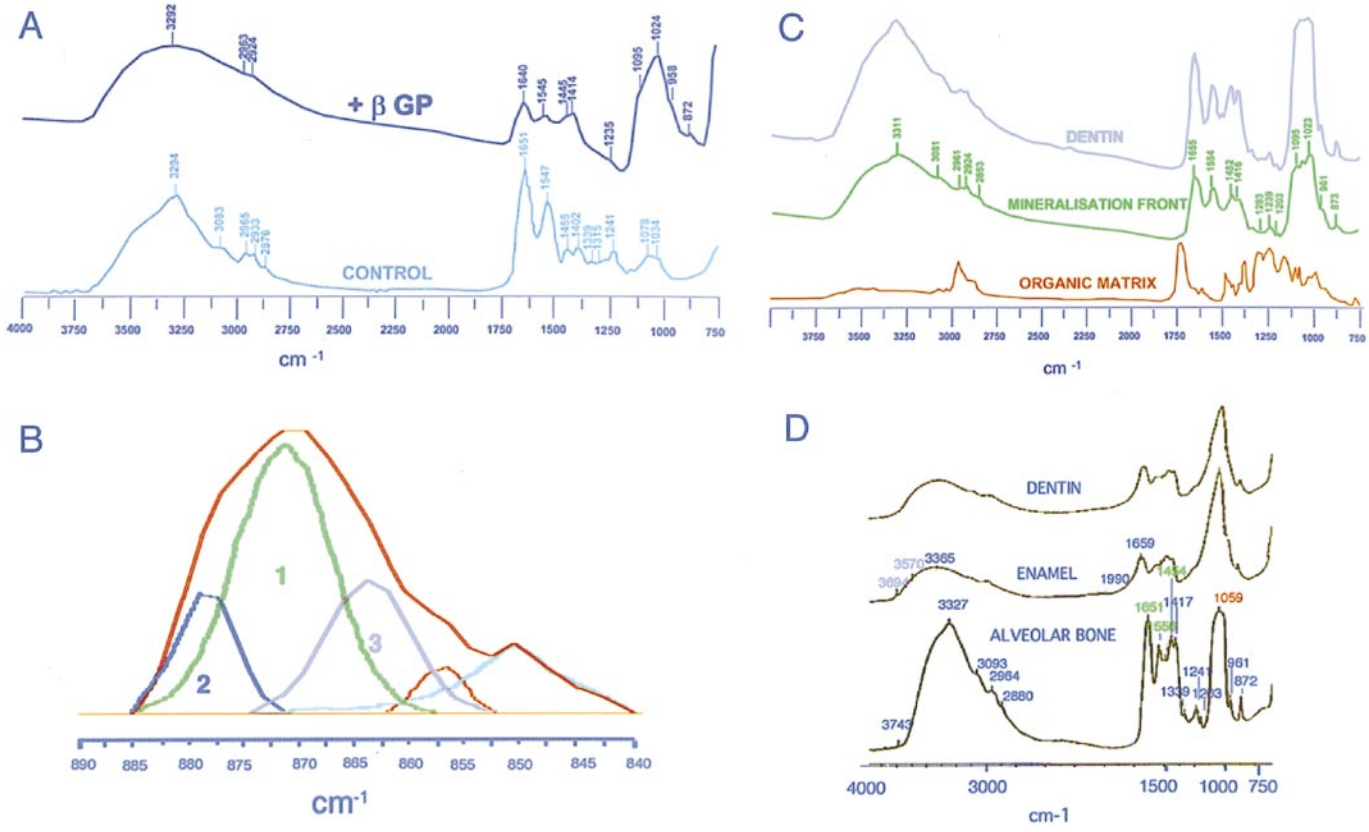

FIG. 3. Fourier transform infrared microspectroscopic examination of the mineralization. (A) The lower spectrum is obtained from untreated cultures *in vitro*. The upper spectrum was obtained from cultures treated with β-glycerophosphate for 4 weeks. It shows identical bands and peaks with wave numbers identical to those obtained *in vivo* at both the organic and the mineral parts of the spectrum of dentin at the mineralization front of dentin. (B) Deconvolution of the v_2 CO_3 band at 872 cm^{-1} obtained *in vitro* after β-glycerophosphate treatment for 4 weeks. It reveals three major components: peak 1 at 872 cm^{-1} represents the maximum and corresponds to carbonate ions located in PO_4 sites; peak 2 at 880 cm^{-1} corresponds exclusively to carbonate ions occupying the monovalent anionic sites of an apatitic structure; and peak 3 at 864 cm^{-1} corresponds to a labile carbonate environment. (C) Dentin *in vivo*. The lower spectrum correlates to the organic matrix without any mineralization. The intermediate spectrum corresponds to the mineralization front and shows peaks at 872, 960, 1024, and 1095 cm^{-1} corresponding to phosphate ions and peaks at 1550 and 1640–1650 cm^{-1} corresponding to amides. The upper spectrum corresponds to the dentin, where all these peaks increased. (D) Mineralization of hard tissues *in vivo*. The upper spectrum corresponds to dentin. The intermediate spectrum corresponds to the enamel and shows characteristic peaks at 3694 and 3750 cm^{-1} corresponding to OH^- ions. The lower spectrum correlates to the alveolar bone. It shows shifts in the amides I and II bands with peaks at 1556 cm^{-1} for the amides II band and at 1651 cm^{-1} for the amides I band. A shift for the $v3$ PO_4^{3-} ions is also observed with a maximum at 1059 cm^{-1} corresponding to type B CO_3.

hibited the OH^- absorption bands at 3570 and 3694 cm^{-1}. In bone (lower spectrum), shifts in amides I and II were observed and PO_4^{-3} ions peak exhibited a maximum at 1059 cm^{-1}.

DISCUSSION

Reciprocal interactions between dental epithelial and mesenchymal tissues lead to the differentiation of mesenchymal cells that line the dental pulp into odontoblasts. These cells are post-mitotic and express specific gene products that form the organic components of the dentin, a unique extracellular mineralized matrix. While the inorganic composition of dentin consists mainly of hydroxyapatite, its organic structure is much more complex. Collagenous and noncollagenous proteins are detected in the dentin. The main collagen found in dentin is the type I collagen (86%), whereas type III, IV, and V collagens are detected in fewer quantities. Dentin noncollagenous proteins such as osteonectin, osteocalcin, osteopontin, and bone sialoprotein have been also localized in bone. However, two proteins have been shown to be tooth-specific: the DSP [9, 10] and the DPP [11]. DSP is a 95-kDa glycoprotein identified within the dentin matrix [43] and accounts for 5–8% of the dentin extracellular matrix. DSP is localized only in dental tissues and its expression is confined to differentiating odontoblasts, with a transient expression in the presecretory ameloblasts [10].

TABLE 1

Comparison of the *in Vitro* Mineralization Components to Those of Dentin and the Attribution of These Components from Literature Values

Wave No. (cm^{-1})	Assignments	Control	βGP	Dentin
872	$\nu 2\ CO_3^{2-}$ ions [34]	None	Well-defined peak	Well-defined peak
960	$\nu 1\ PO_4^{3-}$ ions [35]	None	Shoulder	Well-defined peak
1024	$\nu 3\ PO_4^{3-}$ ions of non stoichiometric apatites [36]	Shoulder	Maximum in a well-defined band	Maximum in a well-defined band
1095	$\nu 3\ PO_4^{3-}$ ions [37]	Shoulder	Shoulder in a well-defined band	Shoulder in a well-defined band
1230	Proteoglycans [38]	Peak	Shoulder	Shoulder
1414	$\nu 3\ CO_3^{2-}$ ions in PO_4^{3-} sites [34]	None	Weak band	Weak band
1445–1545	$\nu 3\ CO_3^{2-}$ ions in OH^- sites [34]	None	Weak double band	Weak double band
1550	Amides II [39, 40]	Strong peak	Weak band	Weak band
1640–1650	Amides I [39–41]	Strong band	Well-defined band	Well-defined band
2879, 2924, 2965	Aliphatic CH_2 [38]	Weak bands	Shoulders	Weak bands
2933, 2963, 3083	Aliphatic CH_3 [38]	Weak bands	Shoulders	Weak band
3292	NH and OH [42]	Broad band	Broad band	Broad band

Note. Despite several shifts in the spectral band positions, the spectrum generated from the *in vitro* mineralization reveals a great analogy with the spectrum generated by the mineralization of the dentin. Control, cultures of pulp cells without β-glycerophosphate; βGP, cultures of pulp cells with β-glycerophosphate.

DPP is synthesized by the odontoblasts and secreted through the odontoblastic process at the mineralization front [11, 12]. DPP is strongly associated with the mineral phase of dentin being soluble only after demineralization of the extracellular matrix. Both DSP and DPP proteins are cleavage products of a single transcript coded by the DSPP gene located on the human chromosome 4 [14]. The intermediate filament protein nestin [31, 32] may be used as an additional marker of differentiated odontoblasts. Our previous studies have shown that nestin is expressed in the developing teeth of rodents [44]. More recently, we have shown that nestin is expressed in odontoblasts of the developing temporary and permanent human teeth. Nestin expression is down-regulated in mature odontoblasts but it is up-regulated after dental injury and in carious lesions [32].

Here we show that cultured human pulp cells are able to differentiate into odontoblast-like cells and to secrete dentin matrix *in vitro*. The differentiation of dental pulp cells into odontoblast-like cells is shown by morphological and most notably by molecular criteria. The cells are polarized in contact with the mineralization nodules, express nestin, and synthesize collagen I, and osteonectin.

TABLE 2

Comparison of the Mineral-to-Matrix Ratios obtained *in Vitro* to That Obtained in Alveolar Bone and Dentin

Control	βGP	Dentin	Alveolar bone
0.35 ± 0.02	4.78 ± 0.03	3.98 ± 0.06	2.5 ± 0.04

Note. This ratio is higher in βGP-treated cultures than in alveolar bone and dentin. Control, cultures of pulp cells without β-glycerophosphate; βGP, cultures of pulp cells with β-glycerophosphate.

The extracellular mineralized matrix secreted by the odontoblast-like cells show the main characteristics of the *in vivo* produced dentin. During dentinogenesis, odontoblastes secrete an unmineralized fibrillar network called predentin. The predentin layer is progressively transformed to dentin as odontoblasts transport and deposit minerals [7]. Thus, the cells recede pulpally while still being connected to the matrix they are synthesizing via odontoblastic processes leading to the formation of tubular morphology of the produced matrix. The transformation of predentine to dentin involves several key regulatory events, which convert the collagen fibers from a noncalcifying matrix to one in which apatite crystals are initiated and grow within and around collagen fibrils [8]. The mechanisms involved in the mineralization of predentin in order to form dentin are not well understood, although several results strongly suggest that the transformation involves the secretion of noncollagenous proteins at the mineralization front [8]. Thus, the deposition of these noncollagenous proteins may result in the initiation and control of mineralization.

Dentin matrix acts as a reservoir of signaling molecules such as members of the TGFβ and FGF super-

families. During dentin decalcification, after a carious irritation, these signaling molecules are released from the matrix and can diffuse to reach the pulp cells. Under the influence of the diffused growth factors, the secretory activity of the odontoblasts is stimulated, leading to the production of the reactionary dentin [23, 32]. However, after deep cavity preparations, the odontoblasts may be disintegrated. Other pulp cells that differentiate into odontoblast-like cells and start the secretion and deposition of a reparative dentin replace the missing odontoblasts [23]. The processes of pulp healing and regeneration can be stimulated by the local application of signaling molecules such as BMP-2, BMP-4, and BMP-7 [45, 46]. However, differentiation of odontoblast-like cells and hard tissue formation have been shown after pulp amputation *in vivo* without the addition of any of these signaling molecules [47]. This may be due to the expression of TGFβ1, BMP-2, BMP-4, and BMP-7 by human pulp cells [48, 49].

In our culture system, the synthesized extracellular matrix molecules formed organic fiber-like structures and these fibrils were the initiation sites of mineral crystal formation. The extracellular matrix continued to deposit and progressively form nodules of mineralized material as demonstrated by Von Kossa stain, while the dental pulp cells remained attached to these nodules with a polarized morphology. Immunohistochemistry revealed that type I collagen was highly expressed in these nodules. In addition, osteonectin which is expressed during human tooth development [3, 50], was deposited during the formation of nodules.

Another interesting aspect is the mineral composition of these nodules. When the FTIR MS spectra obtained from the mineralization nodules *in vitro* were compared with those obtained *in vivo,* they revealed a great analogy with those of the dentin with peaks and bands of the same aspects at the same locations. The βGP spectrum presents the characteristics of the mineralization front of dentin. These characteristics include the wave numbers, their attributions, and the type of peaks and bands.

The deconvolution of the 872-cm^{-1} band of v_2 CO_3^{2-} ions obtained *in vitro* shows that the spectrum is resolved in three major components that correlate well to those described by Rey *et al.* [28]. The 872 band represents the maximum, and corresponds to carbonate ions located in PO_4^{3-} sites [51]. The carbonate ions responsible for the 864 correspond to a labile carbonate environment and the 880 shoulder corresponds exclusively to carbonate ions occupying the monovalent anionic sites of an apatitic structure [34]. This indicates that, despite minor shifts in the peaks localization, the carbonate ions correspond to ones in apatitic structures. Moreover, the mineral-to-organic ratio was higher in the nodules than in the bone, which could be expected, but it was also higher than that of the dentin *in vivo.* This may be due to the absence of the regulation of mineralization *in vitro.*

Moreover, when the mineralization spectra obtained *in vitro* were compared to other tooth hard tissues, major differences were observed when they were compared with the spectra obtained from the enamel and the alveolar bone. The enamel spectra showed the characteristic band of OH^- absorption at 3770 cm^{-1}, which was not observed in the bone and dentin spectra. The alveolar bone spectra revealed shifts in the $v3$ PO_4^{3-} peaks with a maximum at 1059 cm^{-1} correlating to $v3$ PO_4^{3-} ions from type B CO_3, while the maximum obtained *in vitro* and in the dentin spectra was at 1024 cm^{-1} and correlates to nonstoichiometric apatites.

Despite the absence of the tubuli in the matrix produced *in vitro,* these data indicate that the organic as well as the mineral composition of the mineralization nodules obtained *in vitro* has the same composition of dentin, especially at the mineralization front. This is confirmed by several criteria: first, the expression of nestin, which characterizes the secretory odontoblasts; second, the analogy between the FTIR-MS spectra obtained *in vitro* and those of the dentin *in vivo;* third, the big differences observed between the dentin spectra and the enamel and alveolar bone spectra.

In their study, Hao *et al.* [30] have shown that the differentiation of odontoblast-like cells from dental pulp cells and the formation of mineralization nodules in an 8-month embryo could be obtained after the addition of both βGP and ascorbic acid. However, this study is not supported at the molecular level and, in addition, is lacking the analysis of the mineral matrix by FTIR spectrometry. These parameters have been examined in our study. First, we characterized the organic matrix products and the differentiated cells at the molecular level. Second, we studied the mineralized matrix by FTIR microspectroscopy. In addition, we compared the *in vitro*-produced matrix to other mineralized tissues of the tooth, such as the enamel and the alveolar bone.

In our study, the mineralization nodules were obtained in the presence of βGP alone as a source of organic phosphate. This difference may be due to the utilization of embryonic deciduous tooth germ cells not able to synthesize collagen in the absence of ascorbic acid, while the permanent immature third molar cells used here are capable of synthesizing collagen. However, it could be speculated that the addition of ascorbic acid might accelerate the mineralization process in our culture system.

Taken together, these results show that human dental pulp cells of permanent teeth can differentiate *in vitro* into odontoblast-like cells in the presence of βGP alone. These cells secrete a mineralized extracellular matrix showing the molecular and mineral characteristics of the dentin *in vivo.* This system represents a

useful model for the study of many pathological conditions affecting the human teeth leading to reparative dentin production. This could have an important impact for clinical applications.

We thank Dr. JX Lu for help in the osteoblast cells culture. This work was supported by institutional grants from the Université de la Méditerranée and by specific grants of the Ligue Nationale Contre le Cancer and the Association pour la Recherche sur le Cancer (ARC).

REFERENCES

1. Lesot, H., Osman, M., and Ruch, J. V. (1981). Immunofluorescent localization of collagens, fibronectins, and laminin during terminal differentiation of odontoblasts. *Dev. Biol.* **82,** 371–381.
2. Steinfort, J., Van de Stadt, R., and Beertsen, W. (1994). Identification of new rat dentin proteoglycans utilizing C18 chromatography. *J. Biol. Chem.* **269,** 22397–22404.
3. Reichert, T., Störkel, S., Becker, K., and Fisher, L. W. (1992). The role of osteonectin in human tooth development: An immunohistochemical study. *Calcif. Tissue Int.* **50,** 468–472.
4. Bronckers, A. L. J. J., Gay, S., Finkelman, R. D., and Butler, W. T. (1987). Immunolocalization of Gla proteins (osteocalcin) in rat tooth germs: Comparison between indirect immunofluorescence peroxidase–antiperoxidase, avidin–biotin–peroxidase complex and avidin–biotin–gold complex with silver enhancement. *J. Histochem. Cytochem.* **35,** 825–830.
5. Butler, W. T. (1989). The nature and significance of osteopontin. *Connect. Tissue Res.* **23,** 123–136.
6. Chen, J., McCulloch, C. A. G., and Sodek, J. (1993). Bone sialoprotein in developing porcine dental tissues: Cellular expression and comparison of tissue localization with osteopontin and osteonectin. *Arch. Oral. Biol.* **38,** 241–249.
7. Linde, A., and Goldberg, M. (1993). Dentinogenesis. *Crit. Rev. Oral Biol. Med.* **4,** 679–728.
8. Butler, W. T., and Ritchie, H. (1995). The nature and functional significance of dentin extracellular matrix proteins. *Int. J. Dev. Biol.* **39,** 169–179.
9. Ritchie, H. H., Hou, H., Veis, A., and Butler, W. T. (1994). Cloning and sequence determination of rat dentin sialoprotein, a novel dentin protein. *J. Biol. Chem.* **269,** 3698–3702.
10. Butler, W. T., Bhown, M., D'Souza, R. N., Farach-Carson, M. C., Happonen, R.-P., Schrohenloher, R. E., Seyer, J. M., Somerman, M. J., Foster, R. A., Tomana, M., and Van Dijk, S. (1992). Isolation, characterization and immunolocalization of a 53-kDa dentin sialoprotein. *Matrix* **12,** 343–351.
11. MacDougall, M., Zeicher-David, M., and Slavkin, H. C. (1985). Production and characterization of antibodies against murine dentin phosphoprotein. *Biochem. J.* **232,** 493–500.
12. Gorter De Vries, I., Quartier, E., Van Steirtghem, A., Boute, P., Coomans, D., and Wisse, E. (1986). Characterization and immunocytochemical localization of dentine phosphoprotein in rat and bovine teeth. *Arch. Oral Biol.* **31,** 57–66.
13. Ritchie, H. H., and Wang, L. H. (1996). Sequence determination of an extremely acidic rat dentin phosphoprotein. *J. Biol. Chem.* **271,** 21695–21698.
14. MacDougall, M., Simmons, D., Luan, X., Nydegger, J., Feng, J., and Gu, T. T. (1997). Dentin phosphoprotein and dentin sialoprotein are cleavage products expressed from a single transcript coded by a gene on human chromosome 4. *J. Biol. Chem.* **272,** 835–842.
15. Finkelman, R. D., Mohan, S., Jennings, J. C., Taylor, A. K., Jepsen, S., and Baylink, D. J. (1990). Quantitation of growth factors IGF-I, SGF/IGF-II and TGF-B in human dentine. *J. Bone Miner. Res.* **5,** 717–723.
16. Cassidy, N., Fahey, M., Prime, S. S., and Smith, A. J. (1997). Comparative analysis of transforming growth factor-beta isoforms 1–3 in human and rabbit dentine matrices. *Arch. Oral Biol.* **42,** 219–223.
17. Bègue-Kirn, C., Smith, A. J., Loriot, M., Kupferle, C., Ruch, J. V., and Lesot, H. (1994). Comparative analysis of TGFβs, BMPs, IGF, msxs, fibronectin, osteonectin and bone sialoprotein gene expression during normal and *in vitro* induced odontoblast differentiation. *Int. J. Dev. Biol.* **38,** 405–420.
18. Sloan, A. J., and Smith, A. J. (1999). Stimulation of the dentine–pulp complex of rat incisor teeth by transforming growth factor-β isoforms 1–3 *in vitro*. *Arch. Oral Biol.* **44,** 149–156.
19. Sveen, O. B., and Hawes, R. R. (1968). Differentiation of new odontoblasts and dentine bridge formation in rat molar teeth after tooth grinding. *Arch. Oral Biol.* **13,** 1399–1412.
20. Fitzgerald, M., Chiego, D. J., Jr., and Heys, D. R. (1990). Autoradiographic analysis of odontoblast replacement following pulp exposure in primate teeth. *Arch. Oral Biol.* **35,** 707–715.
21. Bergenholz, G. (1981). Inflammatory response of the dental pulp to bacterial irritation. *J. Endodont.* **7,** 100–104.
22. Trowbridge, H. O. (1981). Pathogenesis of pulpitis resulting from dental caries. *J. Endodont.* **7,** 52–60.
23. Tziafas, D., Smith, A. J., and Lesot, H. (2000). Designing new treatment strategies in vital pulp therapy. *J. Dent.* **28,** 77–92.
24. Hu, C. C., Chuhua, Z., Qiubing, Q., and Nanni, B. T. (1998). Reparative dentin formation in rat molars after direct pulp capping with growth factors. *J. Endodont.* **24**(11), 744–751.
25. Rutherford, R. B., Wahle, J., Tucker, M., Rueger, D., and Charette, M. (1993). Induction of reparative dentine formation in monkeys by recombinant human osteogenic protein-1. *Arch. Oral Biol.* **38,** 571–576.
26. Nakashima, M. (1992). The effects of growth factors on DNA synthesis, proteoglycan synthesis and alkaline phosphatase activity in bovine dental pulp cells. *Arch. Oral Biol.* **37,** 231–236.
27. Nakashima, M., Nagasawa, H., Yamada, Y., and Reddi, A. H. (1994). Regulatory role of transforming growth factor-beta, bone morphogenetic protein-2, and protein-4 on gene expression of extracellular matrix proteins and differentiation of dental pulp cells. *Dev. Biol.* **162,** 18–28.
28. Thesleff, I. (1986). Dental papilla cells in culture. Comparison of morphology, growth and collagen synthesis with two other dental-related embryonic mesenchymal cell populations. *Cell Differ.* **18,** 189–198.
29. Satoyoshi, M., Koizumi, T., Teranaka, T., Iwamoto, T., Takita, H., Kuboki, Y., Saito, S., and Mikuni-Takagaki, Y. (1995). Extracellular processing of dentin matrix protein in the mineralizing odontoblast culture. *Calcif. Tissue Int.* **57,** 237–241.
30. Hao, J. J., Shi, J. N., Niu, Z. Y., Xun, W. X., Yue, L., and Xiao, M. Z. (1997). Mineralized nodule formation of human dental papilla cells in culture. *Eur. J. Oral Sci.* **105,** 318–324.
31. Lendahl, U., Zimmerman, L. B., and McKay, R. D. G. (1990). CNS stem cells express a new class of intermediate filament protein. *Cell* **60,** 585–595.
32. About, I., Laurent-Maquin, D., Lendahl, U., and Mitsiadis, T. A. (2000). Nestin expression in embryonic and adult human teeth under normal and pathological conditions. *Am. J. Pathol.* (in press).
33. Lu, J. X., Flautre, B., Anselme, K., Hardouin, P., Gallur, A., Descamps, M., and Thierry, B. (1999). Role of interconnections in porous bioceramics on bone recolonization *in vitro* and *in vivo*. *J. Mater. Sci.* **10,** 111–120.

34. Rey, C., Collins, B., Goehl, T., Dickson, I. R., and Glimcher, M. J. (1989). The carbonate environment in bone mineral: A resolution-enhanced Fourier transform infrared spectroscopy study. *Calcif. Tissue Int.* **45,** 157–164.
35. Gadaleta, S. J., Paschalis, E. P., Betts, F., Mendelsohn, R., and Boskey, A. L. (1996). Fourier transform infrared spectroscopy of the solution mediated conversion of amorphous calcium phosphate to hydroxyapatite: New correlations between x-ray diffraction to infrared data. *Calcif. Tissue Int.* **58,** 9–16.
36. Boskey, A. L., Guidon, P., Doty, S. B., Stiner, D., Leboy, P., and Binderman, I. (1996). The mechanism of B-glycerophosphate action in mineralizing chick limb-bud mesenchymal cell cultures. *J. Bone Miner. Res.* **11,** 1694–1702.
37. Rey, C., Shimizu, M., Collins, B., and Glimcher, M. J. (1991). Resolution-enhanced Fourier transform infrared spectroscopy study of the environment of phosphate ion in the early deposits of a solid phase of calcium phosphate in bone and enamel and their evolution with age: 2 investigations in the $\nu 3\ PO_4$ domain. *Calcif. Tissue Int.* **49,** 383–388.
38. Colthup, N. B., Daly, L. H., and Wiberley, S. E. (1975). Methyl and methylene groups. *In* "Introduction to Infrared and Raman Spectroscopy," pp. 221–233, Academic Press, New York.
39. Kim, H. M., Rey, C., and Glimcher, M. J. (1996). X-ray diffraction, electron microscopy, and Fourier transform infrared spectroscopy of apatite crystals isolated from chicken and bovine calcified cartilage. *Calcif. Tissue Int.* **59,** 58–63.
40. Lazarev, Y. A., Grishkovsky, B. A., and Khromova, T. B. (1984). Amide I band of IR spectrum and structure of collagen and related peptides. *Biopolymers* **24,** 1449–1478.
41. Gadaleta, S. J., Camacho, N. P., Mendelsohn, R., and Boskey, A. L. (1996). Fourier tranform infrared microscopy of calcified turkey leg tendon. *Calcif. Tissue Int.* **58,** 17–23.
42. Rey, C., Miquel, J. L., Facchini, L., Legrand, A. P., and Glimcher, M. J. (1995). Hydroxy groups in bone mineral. *Bone* **16,** 583–586.
43. Ritchie, H. H., Pinero, G. J., Hou, H., and Butler, W. T. (1995). Molecular analysis of rat dentin sialoprotein. *Connect. Tissue Res.* **33,** 395–401.
44. Terling, C., Rass, A., Mitsiadis, T. A., Fried, K., Lendahl, U., and Wroblewski, J. (1995). Expression of the intermediate filament nestin during rodent tooth development. *Int. J. Dev. Biol.* **39,** 947–956.
45. Nakashima, M. (1994). Induction of dentin formation on canine amputated pulp by recombinant human bone morphogenetic proteins (BMP)-2 and -4. *J. Dent. Res.* **73,** 1515–1522.
46. Rutherford, R. B., Wahle, J., Tucker, M., Rueger, D., and Charette, M. (1993). Induction of reparative dentine formation in monkeys by recombinant human osteogenic protein-1. *Arch. Oral Biol.* **38,** 571–576.
47. Van Mullem, P. J. (1991). Healing of the guinea pig incisor after partial pulp removal. *Endod. Dent. Traumatol.* **7,** 164–176.
48. Takeda, K., Oida, S., Goseki, M., Ilmura, T., Matuoka, Y., Amagasa, T., and Sasaki, S. (1994). Expression of bone morphogenetic protein genes in the human dental pulp cells. *Bone* **15,** 467–470.
49. Gu, K., Smoke, R. H., and Rutherford, R. B. (1996). Expression of genes for bone morphogenetic proteins and receptors in human dental pulp. *Arch. Oral Biol.* **41,** 919–923.
50. Shiba, H., Nakamura, S., Shirakawa, M., Nakanishi, K., Okamoto, H., Satakeda, H., Noshiro, M., Kamihagi, K., Katayama, M., and Kato, Y. (1995). Effects of basic fibroblast growth factor on proliferation, the expression of osteonectin (SPARC) and alkaline phosphatase, and calcification in cultures of human pulp cells. *Dev. Biol.* **170,** 457–466.
51. Nelson, D. G. A., and Featherstone, J. D. B. (1982). Preparation analysis and characterization of carbonated apatites. *Calcif. Tissue Int.* **34,** S69–S81.

Received March 22, 2000